Available online at www.sciencedirect.com
SCIENCE DIRECT®
Nuclear Instruments and Methods in Physics Research A 544 (2005) 171–178
NUCLEAR INSTRUMENTS & METHODS IN PHYSICS RESEARCH Section A
www.elsevier.com/locate/nima

Simulation of long-distance beam propagation in the Paul trap simulator experiment ☆

Erik P. Gilson*, Moses Chung, Ronald C. Davidson, Philip C. Efthimion, Richard Majeski, Edward A. Startsev

Plasma Physics Laboratory, Princeton University, Princeton, NJ 08543, USA

Available online 25 February 2005

Abstract

The Paul Trap Simulator Experiment (PTSX) simulates the propagation of intense charged particle beams over distances of many kilometers through magnetic alternating-gradient (AG) transport systems by making use of the similarity between the transverse dynamics of particles in the two systems. One-component pure ion plasmas have been trapped that correspond to normalized intensity parameter $\hat{s} = \omega_p^2(0)/2\omega_q^2 \leqslant 0.8$, where $\omega_p(r)$ is the plasma frequency and ω_q is the average transverse focusing frequency in the smooth-focusing approximation. The PTSX device confines one-component cesium ion plasmas for hundreds of milliseconds, which is equivalent to beam propagation over 10 km. Results are presented for experiments in which the amplitude of the confining voltage waveform has been modified as a function of time. Recent modifications to the device are described, and both the change from a cesium ion source to a barium ion source, and the development of a laser-induced fluorescence diagnostic system are discussed.

PACS: 52.59.Sa; 29.27.−a; 41.85.Ja; 52.27.Jt

Keywords: Ion beam; Accelerator; Plasma; Paul Trap

1. Introduction

As magnetic alternating-gradient (AG) beam transport systems are designed to carry greater amounts of space-charge, it has become increasingly important to understand the non-linear dynamics of intense beam propagation over long distances [1–6]. Specifically, the conditions for quiescent beam propagation, collective mode excitation, generation and dynamics of halo particles, and distribution function effects must be studied. These are key issues for applications where intense beams are required, such as heavy ion fusion, spallation neutron sources, high energy and nuclear physics experiments, and nuclear

☆This research is supported by the U.S. Department of Energy.
*Corresponding author.
E-mail address: egilson@pppl.gov (E.P. Gilson).

0168-9002/$ - see front matter © 2005 Elsevier B.V. All rights reserved.
doi:10.1016/j.nima.2005.01.204

waste transmutation. The Paul Trap Simulator Experiment (PTSX) is a compact laboratory experiment that investigates intense beam dynamics by taking advantage of the similarity between the transverse dynamics of charged particles in the two systems. Here, we summarize the theoretical and experimental underpinnings of the PTSX concept, present initial results on the effect of voltage waveform changes, describe recent device modifications, and discuss planned upgrades to a barium ion source and a laser-induced fluorescence diagnostic system.

2. Relationship to AG focusing systems

Using a linear Paul trap [7] confining a one-component plasma to study the transverse beam dynamics of long charge bunches in AG systems was proposed by Davidson et al. [8] and by Okamoto and Tanaka [9]. The $q\boldsymbol{E}_{\perp}^{\mathrm{ext}}$ forces that the PTSX electrodes exert on the trapped plasma particles are analogous to the transverse $q\boldsymbol{v}_z \times \boldsymbol{B}_{\perp}^{\mathrm{ext}}$ force that the AG system exerts on the beam particles in the beam frame provided that long, coasting beams that are thin relative to the AG system magnet spacing are considered. In fact, for constant beam velocity in linear geometry, the two configurations are related by a Lorentz transformation.

The time dependence of the wall voltage in PTSX corresponds to the spatial dependence of the magnets in an AG system. For an AG system to be useful, it must transport a beam over some reasonable distance, while for PTSX to be useful it must trap a plasma for some suitably long time. Thus, the good confinement properties of one-component ion plasmas in PTSX, and the arbitrary form of the voltage waveform applied to the confining electrodes make PTSX a compact, flexible laboratory facility in which to simulate intense beam propagation through AG systems.

For a thin beam, the applied magnetic field in the AG system may be written as $\boldsymbol{B}_q(\boldsymbol{r}) = B_q'(z)(x\hat{x} - y\hat{y})$. By comparison, the transverse confining potential in PTSX can be expressed as [8]

$$e_b\phi_{\mathrm{ext}}(x,y,t) = \tfrac{1}{2}\kappa_q(t)(x^2 - y^2) \qquad (1)$$

where $\kappa_q(t) = 8e_bV_0(t)/m_b\pi r_w^2$, e_b and m_b are the charge and mass of the trapped particles, $V_0(t)$ is the voltage applied to the trap walls, and r_w is the radius of the cylindrical trap electrodes. The voltage $\pm V_0(t)$ is expressed as $\pm V_{0\ \max}\ g(t)$, where $g(t)$ is a periodic function with unit amplitude and frequency f. For example, to simulate an AG lattice of hard-edged quadrupoles, $g(t)$ would be taken to be a periodic step function. For the work presented here, $g(t) = \sin(2\pi ft)$.

In addition to being able to express the externally applied forces in analogous forms, the self-field forces in both systems can be described by scalar potentials that obey Poisson's equation. The self-field force in PTSX is described by the usual electrostatic potential, whereas the self-field force in an AG system is described by the usual self-electric field ameliorated by the self $\boldsymbol{j} \times \boldsymbol{B}$ force. In PTSX, Poisson's equation determines the evolution of the scalar potential, while in the AG system, Poisson's equation and the $\nabla \times \boldsymbol{B}$ Maxwell equation may be combined into a single Poisson-like equation. In Ref. [8], it was shown that the self-consistent transverse Hamiltonians and the resulting Vlasov equations for the AG system and the PTSX system are equivalent, neglecting end effects.

Beyond the ability of PTSX to study the properties of charged particle beams that travel over large equivalent distances, it is important that PTSX be able to study intense beams. In intense beams, the space-charge effects are non-negligible compared to the emittance effects, and are sufficiently strong that they affect the dynamics of the beam propagation. The strength of the space-charge force is characterized by the plasma frequency $\omega_{\mathrm{p}}^2(r) = n_be_b^2/m_b\varepsilon_0$, whereas the confining force is characterized by the average focusing frequency ω_q of the transverse oscillations of a particle in an AG system [1]. Here, ε_0 is the permittivity of free space, and $n_b(r)$ is the average radial density profile. The normalized intensity parameter $\hat{s} = \omega_{\mathrm{p}}^2(0)/2\omega_q^2$ describes whether the beam is emittance dominated ($\hat{s} \ll 1$) or space-charge dominated ($\hat{s} \to 1$). The depressed phase advance is related approximately to $\hat{s}$ by the relation $\sigma = \sigma_{\mathrm{v}}(1 - \hat{s})^{1/2}$, where σ_{v} is the vacuum phase advance. For example, Fermilab's

Tevatron injector typically operates at $\hat{s} \sim 0.15$ ($\sigma/\sigma_v = 0.92$), and the Spallation Neutron Source is expected to operate at $\hat{s} \sim 0.2$ ($\sigma/\sigma_v = 0.89$). The PTSX device presently operates in the range $0 \leqslant \hat{s} \leqslant 0.8$ ($0.45 \leqslant \sigma/\sigma_v \leqslant 1$). Heavy ion fusion applications will require $\hat{s} \geqslant 0.96$ ($\sigma/\sigma_v \leqslant 0.2$).

3. The PTSX experimental facility

The PTSX device (see Fig. 1) is a linear Paul trap [7] and consists of three co-linear cylinders with radius $r_w = 0.1$ m, each divided into four 90° azimuthal sectors. The cesium-ion plasma is confined radially in the central 2 m long cylinder by the ponderomotive force, as oscillating voltages (typically 235 V at 75 kHz) are applied as shown in Fig. 1. The outer two cylinders are each 0.4 m long and the voltage on these electrodes is held fixed at 150 V in order to confine the plasma axially. To inject or dump the cesium ions, the voltage on one or the other set of outer electrodes is switched to the same oscillating voltage that is applied to the central cylinder. The time duration of injection (t_i), trapping (t_t), and dumping (t_d) may be varied independently with typical values being $t_i = 5$ ms, $t_t \leqslant 300$ ms, and $t_d \geqslant 10$ ms.

Cesium is the ion used in PTSX because of its large mass and its commercial availability. The cesium ion source consists of an aluminosilicate emitter surrounded by a Pierce electrode, followed by an acceleration grid and a deceleration grid to extract the desired ion current and adjust the final ion kinetic energy. This source is centered within the injection electrodes so that the ions are injected far from the fringe fields at the end of the device.

The present diagnostic on PTSX is a Faraday cup on the dumping end of the device. The Faraday cup is moveable in the transverse direction in order to measure the z-integrated radial charge density profile. This is a destructive diagnostic that requires dumping the plasma out of the device each time a measurement is made. The PTSX system is sufficiently reproducible that a complete charge profile can be constructed out of multiple shots where the Faraday cup is repositioned for each shot. The charge collected for a given measurement is typically less than 5 pC and so several hundred plasmas are injected, trapped and dumped in order to reliably measure the signal above the background electrometer noise. In order to reduce ion-neutral collisions, the operating pressure of PTSX is kept below 5×10^{-9} Torr. Then, the ion-neutral collision time is $\nu_{in}^{-1} \sim 1$ s, which is greater than the duration of a typical experiment so that the plasma is collisionless.

Although the governing equations of the AG system and PTSX can be cast into similar forms, it must still be demonstrated through experiment whether or not PTSX can operate under conditions that simulate beam propagation at moderate values of $\hat{s}$ over large equivalent distances. Initial experiments show that this is the case [10]; in PTSX $0 \leqslant \hat{s} \leqslant 0.8$ ($0.45 \leqslant \sigma/\sigma_v \leqslant 1$) and plasmas have been trapped for times that correspond to equivalent propagation distances of 7.5 km.

It is convenient (but not essential) to invoke the smooth-focusing approximation in order to obtain simple analytical expressions for the oscillation

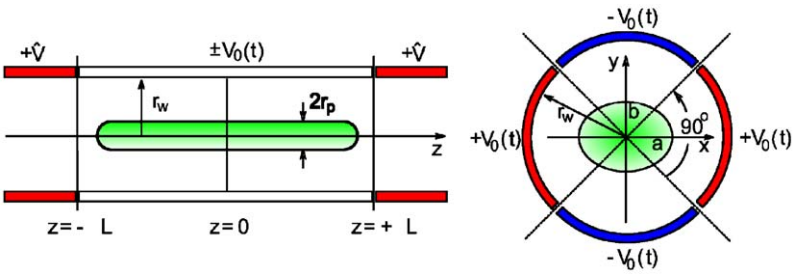

Fig. 1. The PTSX device consists of three cylindrical electrodes with radius $r_w = 0.1$ m, each divided into four 90° sectors. An oscillating voltage $\pm V_0(t)$ confines the plasma in the transverse plane to a radius r_p. Static voltages $+\hat{V}$ on the end electrodes confine the ions axially within a length $2L = 2$ m.

frequency of the average transverse motion ω_q, neglecting space-charge effects [1,9]. In the smooth-focusing approximation, the quadrupolar magnetic field is replaced by a uniform focusing field and the average transverse focusing frequency is given by [1,11,12]

$$\omega_q = \frac{8e_b V_{0\ \max}}{m_b r_w^2 \pi f}\xi \tag{2}$$

where $m_b = 133$ amu for Cs^+ ions in PTSX. The factor ξ depends on the shape of the voltage waveform $g(t)$; $\xi = (2\sqrt{2}\pi)^{-1}$ for a sinusoidal waveform, and $\xi = 4\sqrt{3}/(\eta\sqrt{3-2\eta})$ for a periodic step-function waveform with fill-factor η. Furthermore, the smooth-focusing vacuum phase advance σ_v^{sf} is given by $\sigma_v^{sf} = \omega_q/f$ [1,11,12]. Note that the σ_v^{sf} is a reasonable approximation to the actual vacuum phase advance σ_v found by numerical solution even for moderately large σ_v [1,13]. For example, $\sigma_v = 30^\circ \leftrightarrow \sigma_v^{sf} = 29.7^\circ$, $\sigma_v = 70^\circ \leftrightarrow \sigma_v^{sf} = 65.8^\circ$, and $\sigma_v = 90^\circ \leftrightarrow \sigma_v^{sf} = 81.3^\circ$. Note that the values diverge more rapidly for larger σ_v until $\sigma_v = 180^\circ \leftrightarrow \sigma_v^{sf} = 115.6^\circ$ [13]. The smooth-focusing approximation isakin to the assumptions made in deriving the ponderomotive force that arises from a rapidly oscillating electric field with a spatial gradient.

For the sinusoidal oscillations applied in these particular experiments [10], the transverse equation of motion for single particles in the absence of space-charge is the Matthieu equation. It is well known that when the phase advances exceeds 180° the solutions are unstable. The earliest experiments on PTSX clearly observed this constraint [13,14]. Surfaces of constant σ_v are parabolae in V–f space and for parameters such that $\sigma_v > 180^\circ$ it was not possible to confine particles radially.

The transverse equilibria are the same for AG systems and for PTSX. Under quasi-steady state conditions, for a thermal equilibrium distribution of particles, the average density profile $n_b(r)$ is given by [1,2]

$$n_b(r) = n_b(r=0)\exp\left[-\frac{m_b\omega_q^2 r^2 + 2e_b\phi^s(r)}{2kT}\right]. \tag{3}$$

Here, k is Boltzmann's constant, $T = $ const. is the transverse temperature, and the space-charge potential $\phi^s(r)$ is determined self-consistently from Poisson's equation $r^{-1}\partial_r(r\partial_r\phi^s) = -n_b(r)e_b/\varepsilon_0$. Except for space-charge dominated beams ($\hat{s} \to 1$), numerical solutions of Poisson's equation show that the radial density profile is bell-shaped, and is nearly Gaussian for moderate values of $\hat{s}$ [1]. Regardless of the detailed shape of the density profile, the mean-squared radius of the plasma is determined by the equation

$$m_b\omega_q^2 R_b^2 = 2kT + \frac{N_b e_b^2}{2\pi\varepsilon_0} \tag{4}$$

where $N_b = \int_0^{r_w} n(r)2\pi r\,dr$ is the line density, and $R_b^2 = N_b^{-1}\int_0^{r_w} r^2 n(r)2\pi r\,dr$ is the mean-squared radius. Measurements have shown that, under normal operating conditions, the radial density profile is approximately Gaussian, and the inferred temperature of the plasma is $kT = 0.5$ eV [10].

PTSX must confine plasmas for times that correspond to large transport distances in AG systems. Measurements have demonstrated confinement times of over 100 ms as shown in Fig. 2 [10]. With a frequency f of 75 kHz, this corre-

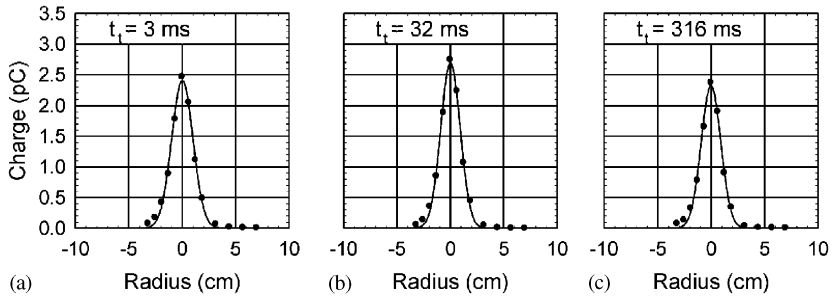

Fig. 2. The radial profile of a trapped plasma with intensity parameter $\hat{s} = 0.18$ ($\sigma/\sigma_0 = 0.90$) is only slightly degraded after 316 ms.

sponds to transport through 7500 equivalent lattice periods.

4. Variable lattice amplitude

Having demonstrated the flexibility of PTSX in simulating the dynamics of intense beam propagation over large distances, modifications of the voltage waveform are now studied. The amplitude $V_{0\ \max}$ is no longer taken to be constant. Generally, the frequency may be allowed to be a time-dependent function $f(t)$. For example, if $f(t) = f(0)V_{0\ \max}(t)/V_{0\ max}(0)$, then ω_q is fixed. Or, if $f(t) = f(0)\sqrt{V_{0\ \max}(t)/V_{0\ \max}(0)}$ then σ_v^{sf} is fixed. In the work presented here, $f(t)$ is taken to be a constant for simplicity, and both ω_q and σ_v^{sf} are then proportional to $V_{0\ \max}$.

Several cases are considered for $V_{0\ \max}(t)$ in order to understand how rapid a change in amplitude can be made without significantly altering the density profile of the plasma. Table 1 summarizes the cases studied: (a) at time t_0, change from $V_{0\ \max} = V_1$ to $V_{0\ \max} = V_2$ for a single period only; (b) change from V_1 to V_2 for all $t > t_0$; (c) vary the amplitude linearly from V_1 to V_2 over a time τ; (d) create a smooth transition of the amplitude of the oscillating wall voltage from V_1 to V_2 according to the function

$$V_{0\ \max}(t) = (V_2 - V_1)\left[\exp\left(\frac{t_{1/2} - t}{\tau}\right) + 1\right]^{-1} + V_1 \quad (5)$$

where $t_{1/2}$ is the time at which the transition is half complete and τ is the characteristic transition time.

Table 1
Four different methods of applying the secondary voltage V_2 are considered to determine their effects on the density profile of the plasma

Case	Lattice change
(a)	$V_{0\ \max} = V_2$ for one period, beginning at $t = t_0$
(b)	$V_{0\ \max} = V_2$ for all $t > t_0$
(c)	Linear ramp from V_1 to V_2 over a time τ
(d)	Smooth ramp from V_1 to V_2 over a time τ

For the data presented here, $V_1 = 235\,\mathrm{V}$ and $f = 75\,\mathrm{kHz}$. For these parameters, $\omega_q = 6.54 \times 10^4\,\mathrm{s}^{-1}$ and $\sigma_v^{sf} = 49.7^\circ$. The one-component plasmas created under these conditions typically have $\hat{s} = 0.22$ ($\sigma/\sigma_v = 0.88$). The plasmas used in these experiments were trapped for 1 ms which is 75 periods of the oscillating wall voltage. For cases (a) and (b), $t_0 = 0.28\,\mathrm{ms}$. For the linear ramp in case (c), $\tau = 1\,\mathrm{ms}$ and the change is made over the entire time that the plasma is trapped. For the smooth ramp in case (d), $t_{1/2} = 0.5\,\mathrm{ms}$, and $\tau = 50\,\mu\mathrm{s}$; for these values, 95% of the transition from V_1 to V_2 occurs during the 366 μs (27 periods) centered about $t_{1/2}$.

Fig. 3 shows the experimental results for $V_2 = 1.6V_1 = 376\,\mathrm{V}$, and a reference charge density profile in which there is no change in the applied wall voltage. For case (a), the central density decreases by a factor of two and many particles are lost. For case (b), the profile has a larger peak signal and is narrower than the reference profile. This is consistent with an increase in the strength of the confining force as characterized by an increased value of ω_q. A scan of t_0 for cases (a) and (b) shows no effect on the resulting density profile. For cases (c) and (d), the profile is further peaked, suggesting that a gradual

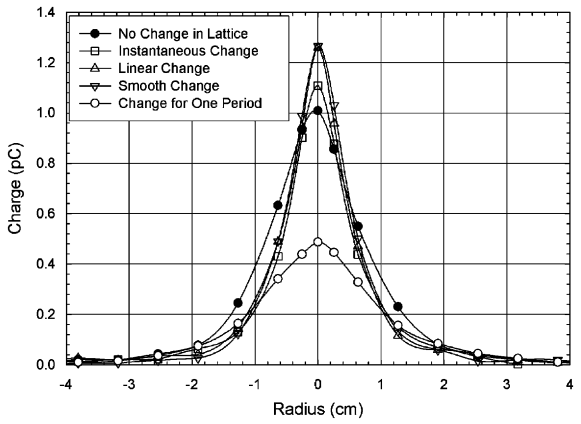

Fig. 3. Increasing the voltage waveform amplitude for only one cycle decreases the amount of plasma trapped. Making the change instantaneously squeezes the plasma somewhat, while either a linear or smooth transition increases the peak signal the most.

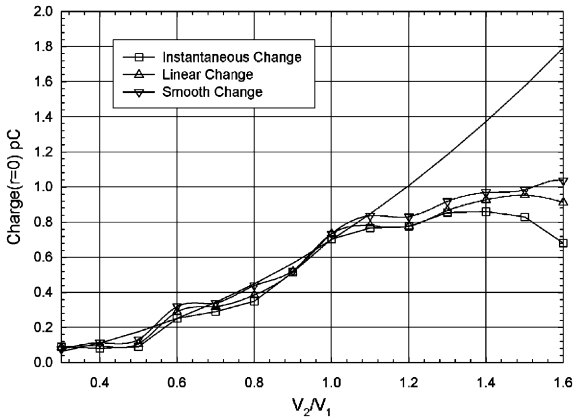

Fig. 4. Decreasing the trap voltage causes the peak density to drop to the same value regardless of how quickly the change is made, and $\hat{s}$ remains unchanged. Increasing the trap voltage increases the peak density, but $\hat{s}$ drops. Smooth changes are more efficient than linear changes, which are in turn more efficient that instantaneous changes.

increase in the applied wall voltage, rather than an instantaneous change, allows the plasma to adiabatically adjust from the initial state to the final state.

The results of varying the amplitude ratio V_2/V_1 over the range 0.3–1.6 are shown in Fig. 4, where the peak signal is plotted versus V_2/V_1 for cases (b)–(d). Although not shown in the figure, experiments for case (a) show that the peak signal decreases regardless of whether V_2 is increased or decreased relative to V_1. The data show that if $V_2/V_1<1$, then the peak signal decreases by approximately the same amount regardless of whether case (b), (c) or (d) is considered. Note that for fixed f, the intensity parameter $\hat{s} \propto n(0)V_{0\,\max}^{-2}$ and so the parabola in Fig. 4 represents a curve of constant $\hat{s}$. For $V_2/V_1<1$ the plasma relaxes while keeping $\hat{s}$ fixed.

The behavior is different if $V_2/V_1>1$. In this case, the abruptness of the transition becomes important, and $\hat{s}$ decreases even while the peak signal generally increases (instantaneous changes at large V_2/V_1 appear to have a deleterious effect as might be anticipated). The more gradual the transition from V_1 to V_2, the larger the peak signal, and $\hat{s}_{(b)}<\hat{s}_{(c)}<\hat{s}_{(d)}$.

5. Device modifications

The original Faraday cup assembly was based on a commercially available Faraday cup that consists of a stack of three 0.75-in. by 1.5-in. plates that supports the cup and had apertures. In order to reduce the effect of stray charge striking the edges of these plates and confounding the measurements, the assembly was enclosed in a copper box that measured 1 in. across by 3 in. tall and that was not symmetrically placed about the collection aperture. This resulted in a boundary condition for the electric potential that varied as the Faraday cup was moved and this was evidenced in the data as an offset in the position of the peak charge density [12].

To assure a boundary condition that was independent of the position of the Faraday cup, a slotted 8-in. diameter copper disk was placed in front of the Faraday cup. Although this eliminated the dependence of the measurement on the position of the Faraday cup, the dumped plasma now broadened significantly as it approached the diagnostic. The time-dependent oscillating voltage that normally confines the plasma radially, gradually becomes a constant axial field in the vicinity of the copper disk, and there is no longer a transverse confining field [13].

A simplified Faraday cup design has now been implemented on PTSX. Fig. 5 shows a schematic of the new collector, and Fig. 6 shows a photograph of the new collector in place in PTSX. The 5 mm diameter head of a copper nail now serves as the collection surface. A coaxial wire is connected to the body of the nail and the wire and nail are inserted into a thin, alumina rod that insulates the

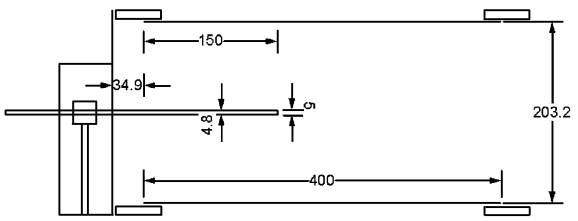

Fig. 5. The new charge collector is a 5 mm diameter copper nail at the end of an arm that places the collector at a null of the potential and fully within the transverse confining field of PTSX away from the fringe fields. All dimensions are in mm.

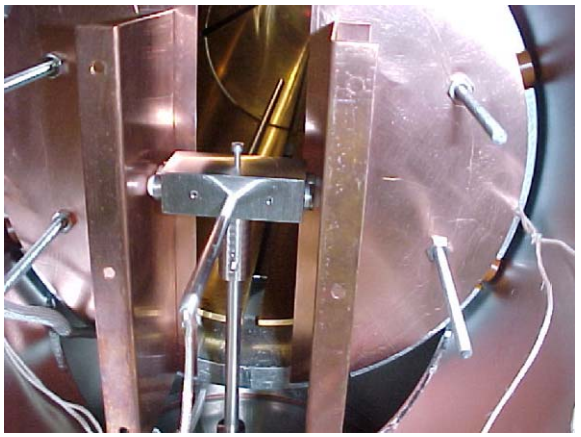

Fig. 6. The new charge collector is guided in the horizontal direction by a pair of cooper plates that are attached to a slotted copper disk at the end of PTSX. These copper structures were originally used for the previous collector design.

collector from the conductive support rod. The ceramic rod, in turn, is inserted into a $\frac{3}{16}$ in. diameter, stainless steel support rod. The base of this rod is clamped into a block that sits atop the arm of the linear motion feedthrough. Thus, the collection surface sits approximately halfway into the dumping electrodes, thereby avoiding fringe fields. Since this thin support rod is grounded and moves in a null of the fully time-dependent voltage $V_0(\boldsymbol{r}, t)$, the new diagnostic has a minimal impact on the potential structure within the dumping electrodes. Measurements show that the radial charge profile no longer exhibits the broadening associated with the equipotential copper disk used previously and is well centered.

In order to make more detailed measurements of the state of the plasma, a more refined diagnostic than the Faraday cup is required. Laser-induced fluorescence is the chosen diagnostic because it can provide four-dimensional transverse phase space information [15]. Furthermore, it is a non-destructive diagnostic with a time resolution that will allow observation of the rapid envelope oscillations of the plasma.

Barium has an atomic structure that makes it well suited for this application and it is slightly heavier than cesium (137 amu versus 133 amu). However, aluminosilicate ions sources for Group II elements do not work as effectively as for the Group I elements. Therefore, a barium source has been designed in which atomic barium vapor contact ionizes on the surface of a refractory metal. When the work function of the ionizing surface exceeds the ionization potential of the atom, then contact ionization is favored at low temperatures according to the Langmuir–Saha equation. If the work function is slightly less than the ionization potential, ionization is favored at high temperature. This type of source is traditionally used in Q-machines and the ionizing surface is further heated to thermionically emit electrons in order to generate a neutral plasma. The temperatures necessary to reach thermionic emission rule out the use metals with low melting points. Because electrons are not wanted in PTSX, platinum, with its high work function, can be used.

Tests performed with metallic barium vapor generated in a 800 °C crucible and directed at a platinum plate heated to ~ 1000 °C have demonstrated microamperes of current. This current is more than adequate for PTSX, and a practical barium ion source is being designed that will meet the system requirements of PTSX.

6. Conclusions

The Paul Trap Simulator Experiment is a compact laboratory experiment that is capable of simulating the transverse dynamics of long, thin charged-particle beams travelling over long distances through alternating-gradient transport systems. Interesting regimes can be studied in which the space-charge of the beam strongly affects the dynamics of the system and in which the beam propagates for over 7500 lattice periods.

Changing the amplitude of the focusing lattice has a variable effect depending on whether the amplitude is increased or decreased and on the abruptness of the change. If the change in amplitude is made for one oscillation cycle only and then the original amplitude is again applied, then the peak density is decreased. For transitions to a smaller final amplitude that are either instantaneous, linear, or smooth, the peak density decreases in such a way as to keep $\hat{s}$ fixed. For transitions to a larger final amplitude, the peak

density increases although $\hat{s}$ decreases, but more so for more abrupt changes. Smooth changes produce the least reduction in $\hat{s}$ while instantaneous changes produce the most. A more systematic exploration of these effects is underway in order to obtain a full understanding of the phenomena.

Modifications have been made to the Faraday cup diagnostic so that the it does not experience the influence of the fringe fields at the end of the device. Also, the smaller cross-section that the collector presents to the system perturbs the orbits of the ions less as they exit the trap. The design of a barium ion source will allow for the implementation of a laser-induced fluorescence system that will allow the full four-dimensional transverse phase space to be measured.

References

[1] R.C. Davidson, H. Qin, Physics of Intense Charged Particle Beams in High Intensity Accelerators, World Scientific, Singapore, 2001.
[2] M. Reiser, Theory and Design of Charged Particle Beams, Wiley, New York, 1994.
[3] A.W. Chao, Physics of Collective Beam Instabilities in High Energy Accelerators, Wiley, New York, 1993.
[4] See, for example, Proceedings of the 2001 Particle Accelerator Conference (IEEE Catalog Number 01CH37268), pp. 1–4098.
[5] P.G. O'Shea, M. Reiser, R.A. Kishek, S. Bernal, H. Li, M. Pruessner, V. Yun, Y. Cui, W. Zhang, Y. Zou, et al., Nucl. Instr. and Meth. A 464 (2001) 646.
[6] N. Kjærgaard, M. Drewsen, Phys. Plasmas 8 (2001) 1371.
[7] W. Paul, H. Steinwedel, Z. Naturforsch. A 8 (1953) 448.
[8] R.C. Davidson, H. Qin, G. Shvets, Phys. Plasmas 7 (2000) 1020.
[9] H. Okamoto, H. Tanaka, Nucl. Instr. and Meth. A 437 (1999) 178.
[10] E.P. Gilson, R.C. Davidson, P.C. Efthimion, R. Majeski, Phys. Rev. Lett. 92 (2004) 155002.
[11] E.P. Gilson, R.C. Davidson, P.C. Efthimion, R. Majeski, H. Qin, Laser Part. Beams 21 (2003) 549.
[12] E.P. Gilson, R.C. Davidson, P.C. Efthimion, R. Majeski, H. Qin, in: Proceedings of the 2003 Particle Accelerator Conference (IEEE Catalog No. 03CH37423C, 2003), p. 2655.
[13] E.P. Gilson, R.C. Davidson, P.C. Efthimion, R. Majeski, E.A. Startsev, American Institute of Physics Conference, Proceedings, vol. 692, 2003, pp. 211.
[14] C.M. Celata, F.M. Bieniosek, E. Henestroza, J.W. Kwan, E.P. Lee, G. Logan, L. Prost, P.A. Seidl, J.-L. Vay, W.L. Waldron, et al., Phys. Plasmas 10 (2003) 2064.
[15] M. Chung, E.P. Gilson, R.C. Davidson, P.C. Efthimion, R. Majeski, E.A. Startsev, Nucl. Instr. and Meth., those proceedings, 2004.